Functional Polystyrene Derivatives Influence the Miscibility and Helical Peptide Secondary Structures of Poly(gamma-benzyl L-glutamate)

ARTICLE *in* MACROMOLECULES · MARCH 2012

Impact Factor: 5.8 · DOI: 10.1021/ma300061w

2 AUTHORS, INCLUDING:

Shiao-Wei Kuo
National Sun Yat-sen University
267 PUBLICATIONS **5,591** CITATIONS

Macromolecules

Article

pubs.acs.org/Macromolecules

Functional Polystyrene Derivatives Influence the Miscibility and Helical Peptide Secondary Structures of Poly(γ-benzyl L-glutamate)

Shiao-Wei Kuo* and Chi-Jen Chen

Department of Materials and Optoelectronic Science, Center for Nanoscience and Nanotechnology, National Sun Yat-Sen University, Kaohsiung, Taiwan

ABSTRACT: We synthesized polystyrene (PS) and poly(acetoxystyrene) (PAS) homopolymers through atom transfer radical polymerization (of styrene and 4-acetoxystryene monomers, respectively) and then prepared poly(vinylphenol) (PVPh) through acetoxyl hydrazinolysis of PAS with hydrazine monohydrate. To investigate the influences of these three functionalized polystyrene derivatives on the helical peptide secondary structures and miscibility behavior of polypeptide homopolymers, we blended PS, PAS, and PVPh with a low-molecular-weight poly(γ-benzyl L-glutamate) (PBLG) homopolymer and analyzed these blends using differential scanning calorimetry (DSC), Fourier transform infrared (FTIR) spectroscopy, solid state nuclear magnetic resonance (NMR) spectroscopy, and wide-angle X-ray diffraction (WAXD). Variations in the intermolecular interactions (e.g., π−π, dipole−dipole, hydrogen bonding) strongly affected the miscibility behavior and secondary structures of PBLG. The weak π−π interactions between PS and PBLG resulted in only partial miscibility, with the α-helical secondary structure of PBLG remaining almost unchanged upon increasing the content of the PS homopolymer; in contrast, the stronger dipole−dipole interactions between PAS and PBLG and the hydrogen-bonding interactions between PVPh and PBLG led to complete miscibility, with the content of α-helical PBLG secondary structures increasing upon increasing the contents of both the PAS and PVPh homopolymers. Because the hydrogen-bonding interactions in the PVPh/PBLG blends were stronger than the dipole−dipole interactions in the PAS/PBLG blends, the fractions of α-helical secondary structures in the PVPh/PBLG systems were larger than those in the PAS/PBLG systems. Indeed, the contents of α-helical conformations in these three blend systems correlated strongly with the strength of their intermolecular interactions.

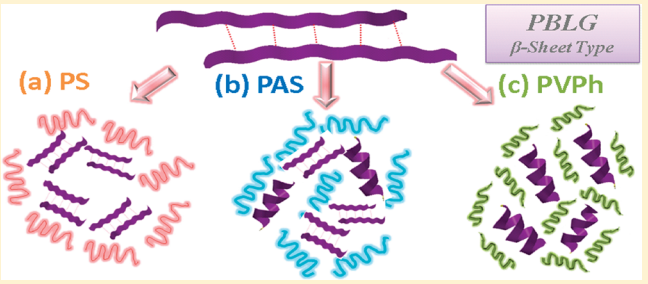

INTRODUCTION

The α-helical structures of polypeptides [e.g., poly(γ-benzyl L-glutamate) (PBLG)] result in the formation of rigid rod structures that can exhibit liquid crystalline ordering in concentrated solutions and cast films.[1−3] PBLG, which has been commercially available since the 1950s,[4] is often employed as a model rigid rod system in solution and in the solid state,[5−7] providing unique bulk (e.g., thermotropic liquid crystalline ordering)[8,9] and solution (thermoreversible gelation)[10−13] behavior. PBLG also forms hierarchically ordered structures containing α-helices, which can be regarded as rigid rods, stabilized through intramolecular hydrogen-bonding interactions, and β-sheets, stabilized by intermolecular interactions, as fundamental secondary motifs.[14] Conformational studies of model polypeptides are necessary if we are to mimic the biological activity of more-complex proteins because the secondary structures of peptide chains influence the formation of proteins with well-defined tertiary structures.[15]

For several decades, most of the methods for synthesizing poly(peptide-*b*-nonpeptide) (rod/coil) block copolymers, with potential applications in tissue engineering and drug delivery, have followed Nature's strategies for producing supramolecular bioactive assemblies.[16−31] These systems can exhibit significant stabilization of the α-helical secondary structures relative to those of the corresponding PBLG oligomers; for example, in the Fourier transform infrared (FTIR) spectra of poly(styrene-*b*-γ-benzyl L-glutamate) (PS-*b*-PBLG) copolymers reported by Klok et al.[16] The synthesis of diblock copolymers is, however, a difficult and time-consuming means of varying the secondary structure of a polypeptide. From practical and economical points of view, physical blending is a simpler and more effective method for modifying a polypeptide or any other useful material, with greater versatility and flexibility, than through the development of new polymers.[32−36] From a previous study,[37] we reported that the secondary structures of the polypeptides poly(γ-methyl L-glutamate) (PMLG), poly(γ-ethyl L-glutamate) (PELG), and PBLG could be altered through blending with other random-coil nonpeptide oligomers (in that case, phenolic resin), mediated by hydrogen-bonding interactions. We found that the α-helical conformation in these three blend systems correlated strongly with the rigidity of side chain groups of the polypeptides and the strength of the intermolecular hydrogen bonding with the phenolic resin.[37]

Received: January 9, 2012
Revised: February 12, 2012
Published: February 22, 2012

   dx.doi.org/10.1021/ma300061w | *Macromolecules* 2012, 45, 2442−2452

In this present study, we investigated the influence of three functionalized polystyrene derivatives (homopolymers) on the peptide secondary structure and miscibility behavior of PBLG. We synthesized polystyrene (PS) and poly(acetoxystyrene) (PAS) homopolymers through atom transfer radical polymerizations of styrene and 4-acetoxystryene, respectively, and then prepared poly(vinylphenol) (PVPh) through acetoxyl hydrazinolysis of PAS with hydrazine monohydrate. We expected weak $\pi-\pi$ interactions to exist between PS and PBLG, moderate dipole−dipole interactions between PAS and PBLG,[38−40] and strong hydrogen-bonding interactions between PVPh and PBLG, with the strength of the intermolecular interactions in the blends increasing in the order PVPh/PBLG > PAS/PBLG > PS/PBLG. Changing the functionality of the polystyrene derivative is a simple approach toward distinguishing the influence of intermolecular interactions on the miscibility behavior and secondary structure of PBLG. We have used differential scanning calorimetry (DSC), FTIR spectroscopy, solid state nuclear magnetic resonance (NMR) spectroscopy, and wide-angle X-ray diffraction (WAXD) to investigate the miscibility behavior, hydrogen-bonding interactions, and secondary structures of these three binary blends.

EXPERIMENTAL SECTION

Materials. Butylamine was purchased from Tokyo Kasei Kogyo, Japan. γ-Benzyl L-glutamate *N*-carboxyanhydride (BLG NCA) monomer was prepared according to a literature procedure[41] and stored at −30 °C. Styrene and 4-acetoxystyrene (Aldrich) were vacuum-distilled over CaH_2 and stored under N_2 at −10 °C. Copper(I) bromide (CuBr) was purified by washing sequentially with glacial AcOH (overnight), absolute EtOH, and Et_2O and then drying under vacuum. *N*,*N*-Dimethylformamide (DMF), 1-phenylethyl bromide, and *N*,*N*,*N*′,*N*′,*N*″-pentamethyldiethylenetriamine (PMDETA, 99%) were purchased from Aldrich. All solvents were distilled prior to use.

PBLG.[37] In a typical experiment, the BLG NCA monomer (2 g) was weighed in a glovebox under pure Ar, placed in a flame-dried Schlenk tube, and dissolved in anhydrous DMF (40 mL). The solution was stirred for 10 min, and then butylamine (50 μL) was added using a N_2-purged syringe. After stirring the solution for 40 h at room temperature, the polymer was recovered through precipitation in Et_2O and dried under high vacuum.

PS and PAS.[42,43] CuBr (green powder) was added to a reactor and degasser operated under vacuum, followed by dry styrene (or acetoxystyrene) and (1-bromoethyl)benzene (by syringe) as the monomer and initiator, respectively. The mixture was subjected to at least two freeze/pump/thaw cycles. The ligand PMDETA was added via syringe under Ar, and then the system was once again subjected to the freeze/pump/thaw procedure. The reactor was placed in an oil bath and heated at 110 °C for 2 h. When the reaction was complete, the mixture was diluted with THF and passed through a neutral alumina column to remove the catalyst. The polymer solution was concentrated under rotary evaporation. The polymer was precipitated with MeOH and collected by filtration. The white powder of PS (or PAS) was dried under vacuum.

PVPh.[42,43] In a typical procedure, the PAS (7.2 mmol of AS) homopolymer was dissolved in 1,4-dioxane (30 mL), and then hydrazine hydrate (3 mL) was added via syringe (volume ratio of hydrazine hydrate to 1,4-dioxane, 1:9). The reaction mixture was maintained at room temperature under an Ar atmosphere for 10 h. The solution was concentrated, washed several times with deionized H_2O, and then dried in a vacuum oven at room temperature for 72 h.

Blend Preparations. Mixtures of PS/PBLG, PAS/PBLG, and PVPh/PBLG at various blend compositions were prepared through solution casting. A DMF solution containing 5 wt % of the polymer mixture was stirred for 6−8 h, and then the solvent was evaporated slowly at 50 °C for 1 day. The film of the blend was then dried at 80 °C for 2 days to ensure total removal of residual solvent.

Characterization. ^{1}H NMR spectra were recorded at room temperature using a Bruker AM 500 (500 MHz) spectrometer, with the residual proton resonance of the deuterated solvent as the internal standard. High-resolution solid state NMR spectra were recorded at room temperature using a Bruker DSX-400 spectrometer operated at resonance frequencies of 399.53 and 100.47 MHz for ^{1}H and ^{13}C nuclei, respectively. ^{13}C cross-polarization (CP)/magic angle sample spinning (MAS) spectra were measured using a 3.9 μs 90° pulse, a 3 s pulse delay time, a 30 ms acquisition time, and 2048 scans. All NMR spectra were recorded at 300 K using broad band proton decoupling and a normal CP pulse sequence. An MAS rate of 5.4 kHz was used to avoid absorption overlapping. Differential scanning calorimetry (DSC) was performed using a TA-Q20 instrument operated at a scan rate of 10 °C/min over the temperature range from −90 to 200 °C under a N_2 atmosphere. FTIR spectra of the polymer films were recorded using a Bruker Tensor 27 FTIR spectrophotometer with the conventional KBr disk method; 32 scans were collected at a spectral resolution of 1 cm^{-1}. Because polymers containing OH groups are hygroscopic, pure N_2 gas was used to purge the spectrometer's optical box to ensure dry sample films. X-ray diffraction (XRD) data were collected on the wiggler beamline BL17A1 of the National Synchrotron Radiation Research Center (NSRRC), Taiwan. A triangular bent Si (111) single crystal was employed to obtain a monochromated beam having a wavelength (λ) of 1.330 01 Å. The XRD patterns were collected using an imaging plate (IP; Fuji BAS III; area = 20 × 40 cm^2) curved with a radius equivalent to the sample-to-detector distance (280 mm). The two-dimensional (2D) XRD patterns of the samples (typical diameter: 10 mm; thickness: 1 mm) were circularly averaged to obtain one-dimensional (1D) diffraction profiles $I(Q)$. The values of Q were calibrated using standard samples of silver behenate and Si powder (NBS 640b).

Table 1. Molecular Characteristics of PBLG, PS, PAS, and PVPh

polymer	M_n	PDI	DP	T_g (°C)
PBLG	1370	1.06	6	23
PS	6270	1.07	60	83
PAS	8910	1.12	55	122
PVPh	6600	1.12	55	170

RESULTS AND DISCUSSION

Table 1 and Scheme 1 summarize the molecular weights, thermal properties, and chemical structures of the PBLG, PS, PAS, and PVPh homopolymers prepared in this study.

FTIR Spectra of PS, PAS, and PVPh. Figure 1 presents FTIR spectra of the PS, PAS, and PVPh homopolymers at room temperature. The bands for PS appear at 3002−3100 cm^{-1}, due to C−H stretching vibrations of the aromatic rings, and 1600 cm^{-1}, due to C═C bending vibrations of the aromatic rings (Figure 1a). In the spectrum of PAS (Figure 1b),[44,45] the absorption at 1763 cm^{-1} is assigned to the C═O unit; the absorptions of the aromatic rings are similar to those in the spectrum of PS. The C═O group absorption at 1760 cm^{-1} in Figure 1b disappeared completely after deacetylation, but a broad absorbance from the OH groups of the PVPh homopolymer appeared between 3100 and 3700 cm^{-1} (Figure 1c).[46−48]

Thermal Analyses of Polymer Blends. Thermal characterization of polymer blends is a common method for

dx.doi.org/10.1021/ma300061w | Macromolecules 2012, 45, 2442−2452

Scheme 1. Chemical Structures of PS, PAS, PVPh, and PBLG

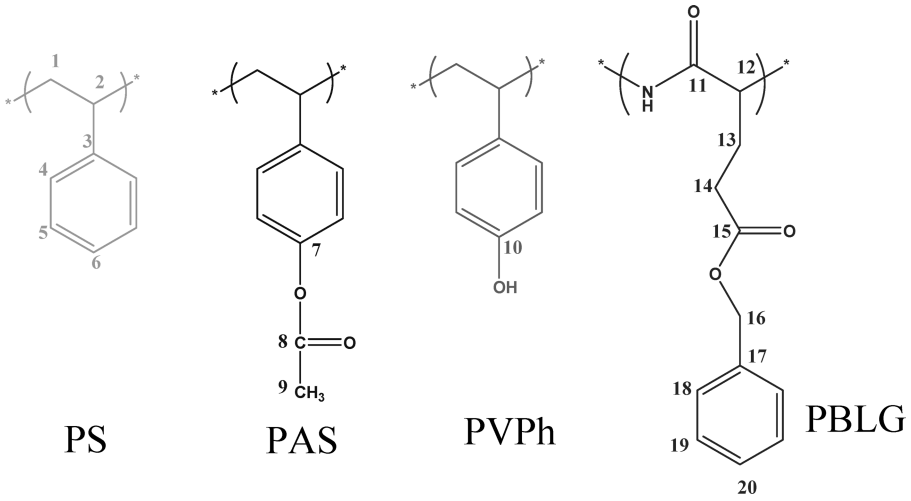

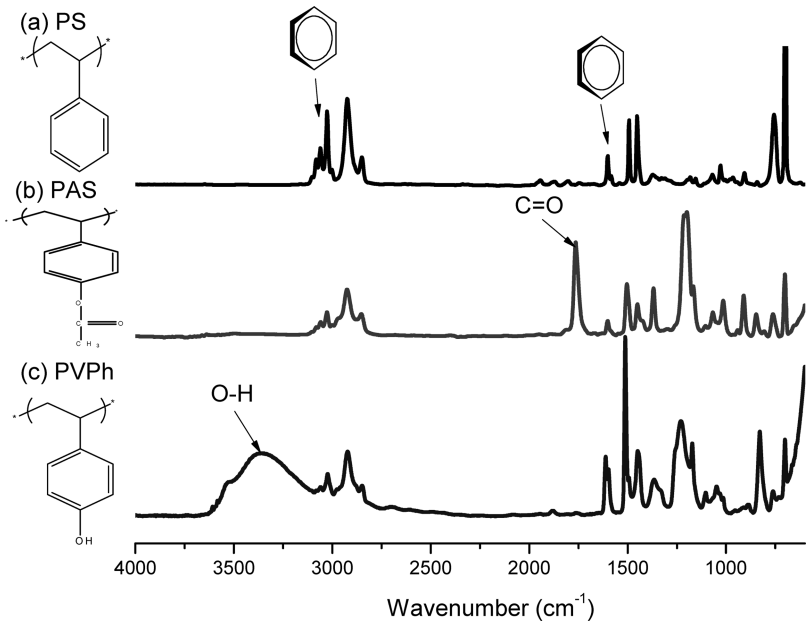

Figure 1. FTIR spectra (recorded at room temperature) of the PS, PAS, and PVPh homopolymers.

determining the miscibility of polymer blends. Some miscible blends can show a dual glass temperature with a relatively large T_g difference between two homopolymers with weak intermolecular interactions.[49,50] In this study, we found it difficult to observe the glass transition temperatures (T_g) of the polypeptides having rigid conformations and well-defined secondary structures (helices, sheets).[51] The value of T_g of pure PBLG is reported to be 23 °C;[14] in this present study, we obtained values of T_g for pure PS, PAS, and PVPh of 83, 122, and 170 °C, respectively. Because the glass transition behavior is strongly dependent on the molecular weight, the value of T_g (83 °C) for the PS (M_n = 6270 g/mol) used in this study was lower than those reported previously for high-molecular-weight PS (T_g = 100 °C).[52,53] Figure 2 presents the second heating runs in our DSC analyses of PBLG blends with PS, PAS, and PVPh at various compositions. The DSC thermograms of the PS/PBLG blend (Figure 2a) displays two values of T_g, implying that the components were phase-separated in the amorphous phase. The value of T_g of the PBLG domain remained almost unchanged upon increasing the content of the PS homopolymer; in contrast, the value of T_g of the PS domain decreased upon increasing the PBLG content (Figure 3a), indicating that the PS segment was partially miscible in the PBLG matrix as a result of $\pi-\pi$ interactions (Scheme 2a). This observation is similar to that for the microphase separation that occurs in PS-*b*-PBLG diblock copolymers.[16] All of our PAS/PBLG and PVPh/PBLG blends exhibited a single glass transition temperature over the entire range of blend compositions. The single value of T_g strongly suggested that these blends were fully miscible and possessed homogeneous amorphous phases. In addition, the values of T_g of the PAS/PBLG (Figure 3b) and PVPh/PBLG (Figure 3c) blends both decreased upon increasing their PBLG contents. As a result, we conclude that PAS and PVPh are miscible with PBLG, whereas PS is only partially miscible with PBLG. The miscibility of the PVPh/PBLG blend is inconsistent with the results reported by Painter et al.[14,32] They found that PBLG, with its flexible side chains, adopted an α-helical rigid rod conformation because of its high molecular weight (M_n = 248 000 g/mol); on the basis of FTIR spectroscopic analyses, they did not observe the presence of

dx.doi.org/10.1021/ma300061w | *Macromolecules* 2012, 45, 2442−2452

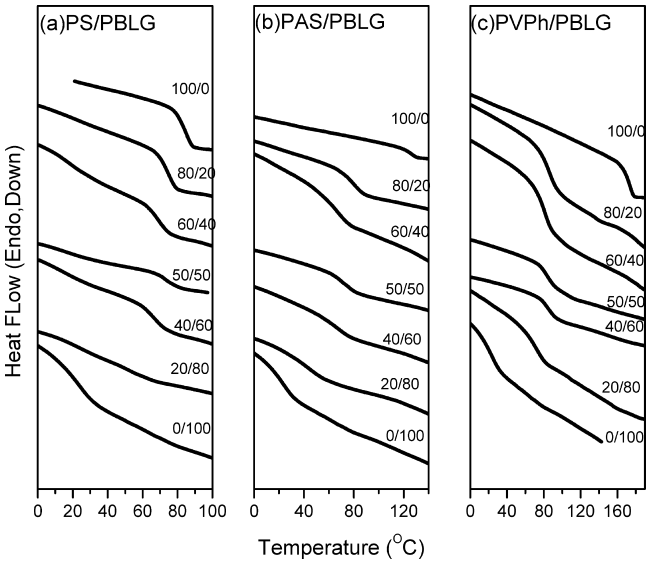

Figure 2. DSC traces (second heating run) of (a) PS/PBLG, (b) PAS/PBLG, and (c) PVPh/PBLG blends.

intermolecular hydrogen bonds between the C═O groups on the side chains of PBLG and the OH groups of PVPh, indicating that the system was immiscible and phase-separated.[32] Our conflicting observations presumably arose from the much lower molecular weight of the PBLG (1370 g/mol) used in this study, relative to that (248 000 g/mol) used previously, with the lower degree of polymerization (DP) increasing the entropic terms, which much more like solutions of PAS, and PVPh in the solvent PBLG$_6$, and, thereby, enhancing the miscibility of the polymer blend system.[54] In addition, at a low DP (e.g., <18 in this case), three secondary structures (α-helix, β-sheet, random coil) are present for PBLG; when the DP increases, however, the rigid α-helical secondary structure is favored.[14,32] As a result, the more-flexible secondary structures—β-sheet and random coil—might have a greater possibility to form intermolecular hydrogen bonds with PVPh than would the rigid α-helical conformation, contributing significantly to the enthalpic term.[54]

FTIR Spectroscopic Analyses of Polymer Blends. FTIR spectroscopy can provide information relating to the specific interactions between polymers, both qualitatively and quantitatively. The NH and OH stretching ranges in a FTIR spectrum are sensitive to the degrees of intermolecular interaction. Figure 4 displays FTIR spectra (in the range 2700−4000 cm^{-1}) of PS/PBLG, PAS/PBLG, and PVPh/PBLG blends, recorded at room temperature. For pure PBLG, we observe a sharp band at 3290 cm^{-1}, representing the NH stretching (primary amine) vibrations of the polypeptide. The characteristics of this sharp band remained unchanged upon increasing the PS, PAS, and PVPh contents, indicating that no hydrogen-bonding interactions occurred between these three homopolymers and the NH groups of PBLG. The FTIR spectrum of pure PVPh featured two distinct bands in the OH stretching region: a very broad band centered at 3350 cm^{-1}, representing the wide distribution of hydrogen-bonded OH groups, and a sharp band at 3525 cm^{-1}, representing free OH groups. The intensity of the signal for the free OH groups decreased upon increasing the PBLG content. Meanwhile, the broad signal of the hydrogen-bonded OH groups shifted to higher frequency upon increasing the PBLG content, suggesting a switch from strong intramolecular OH···OH (PVPh/PVPh) hydrogen bonds into weak intermolecular OH···O═C (PVPh/PBLG) hydrogen bonds.[55,56]

Figure 5 presents FTIR spectra recorded at room temperature to obtain information regarding the secondary structures of the PS/PBLG, PAS/PBLG, and PVPh/PBLG blends. Analyzing these spectra using the second derivative technique,[17] we observed six major peaks for pure PBLG, representing the free C═O group (1735 cm^{-1});[32] the secondary structures of the amide I groups in random coil (1692 cm^{-1}),[17] α-helical (1655 cm^{-1}),[16] and β-sheet (1626 cm^{-1})[16] conformations; and the stretching of benzene units (1610 and 1594 cm^{-1}). For our analysis, we ignored the signals for the random-coil amide I groups at 1640−1650 and 1660−1670 cm^{-1} because many bands made it difficult to calculate the

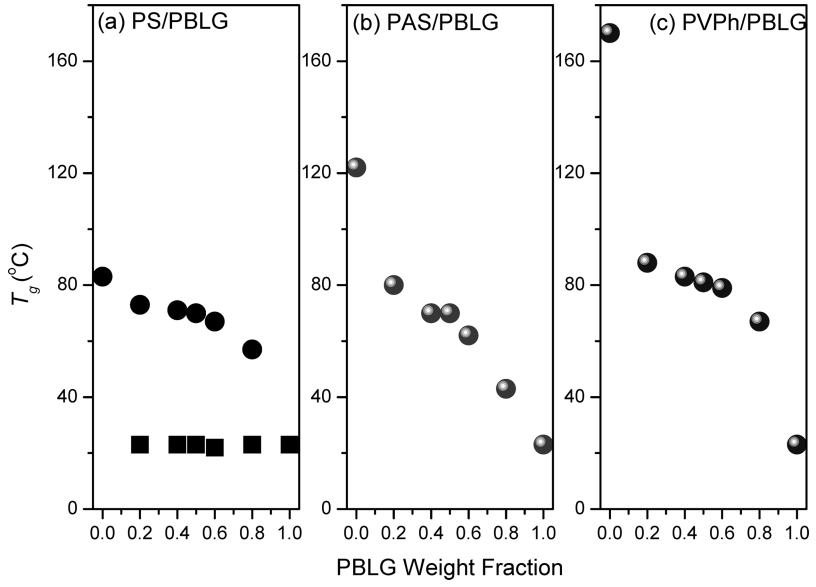

Figure 3. Glass transition temperatures plotted with respect to the PBLG weight fraction in (a) PS/PBLG, (b) PAS/PBLG, and (c) PVPh/PBLG blends.

dx.doi.org/10.1021/ma300061w | Macromolecules 2012, 45, 2442−2452

Scheme 2. Possible Morphologies, Secondary Structures, and Intermolecular Interactions of PBLG Blended with PS, PAS, and PVPh Homopolymers

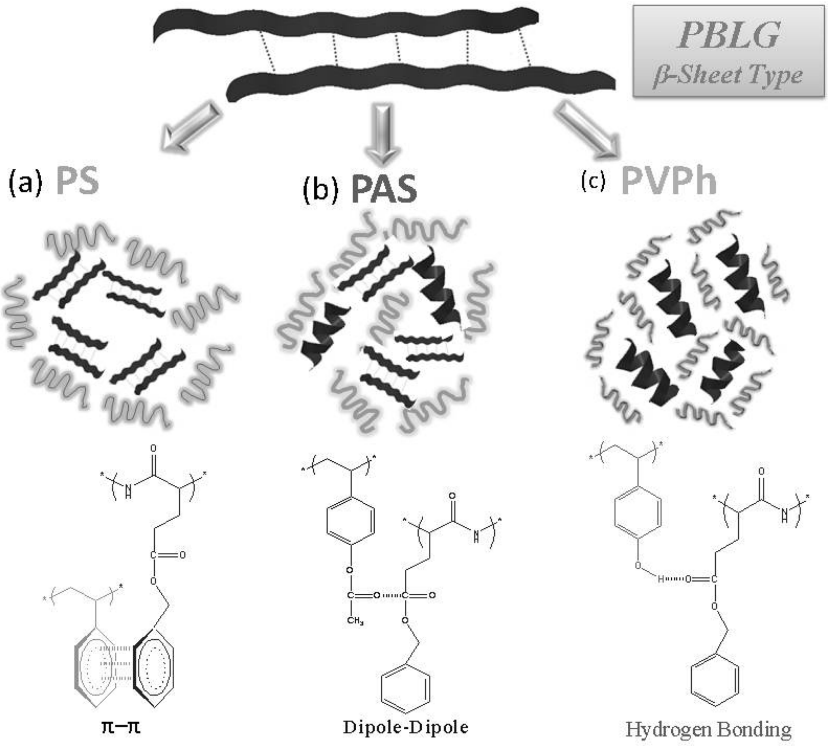

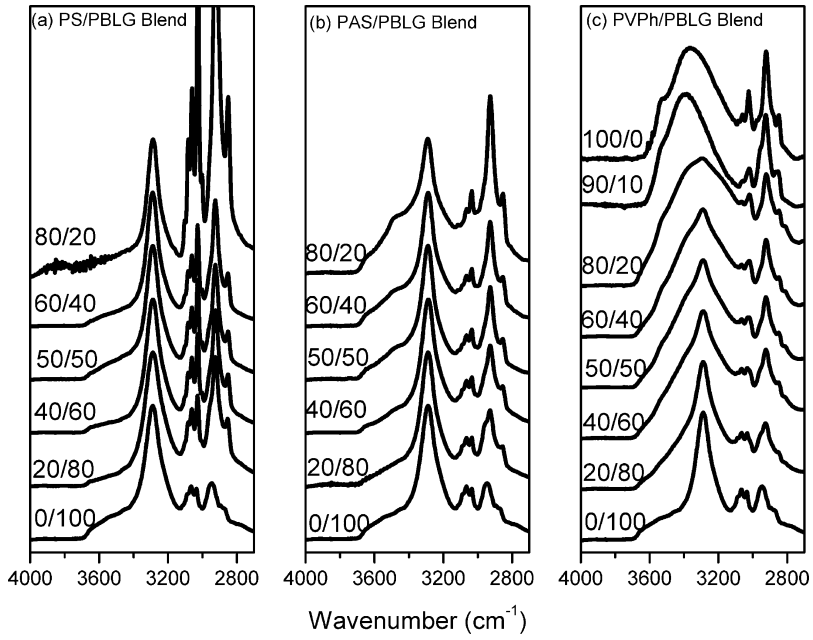

Figure 4. FTIR spectra (4000–2700 cm^{-1}, recorded at room temperature) of the (a) PS/PBLG, (b) PAS/PBLG, and (c) PVPh/PBLG blends.

quantitative area fractions of the secondary structures.[57] After blending with the PS homopolymer, the positions of these six major peaks did not change, with only the intensity of the stretching band for the benzene units at 1600 cm^{-1} increasing upon increasing the PS content. For the PAS/PBLG blends, a new signal for free C═O groups appeared at 1760 cm^{-1}, representing the PAS segment. After blending with the PVPh homopolymer, however, a new signal for hydrogen-bonded C═O units appeared at 1710 cm^{-1}, indicating that hydrogen bonding existed between the C═O groups of PBLG and the OH groups of PVPh. For deconvolution, we fitted a series of Gaussian distributions (Figure 6) to quantify the fractions of each of the peaks. Table 2 and Figures 7 and 8 summarize the curve-fitting data for the amide I groups of the β-sheet, α-helical, and random coil structures of PBLG and for the free and hydrogen-bonded C═O units in the PBLG blends with the PVPh homopolymer. Figure 7 plots the fraction of hydrogen-bonded C═O groups of PBLG with respect to the

dx.doi.org/10.1021/ma300061w | Macromolecules 2012, 45, 2442–2452

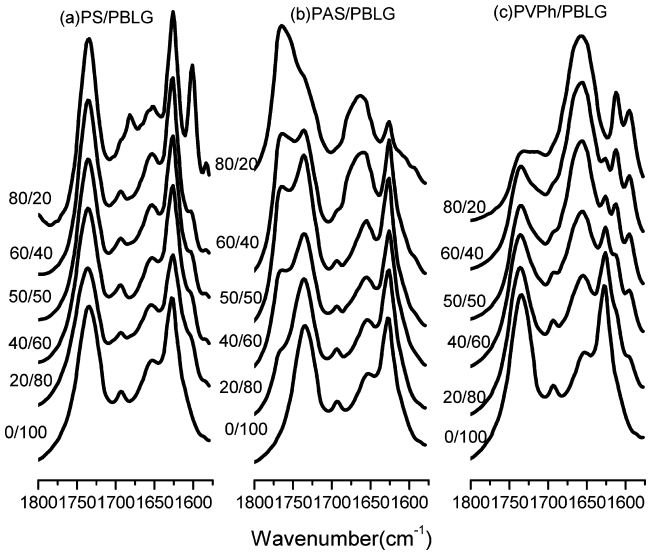

Figure 5. FTIR spectra (1800−1580 cm^{-1}, recorded at room temperature) of the (a) PS/PBLG, (b) PAS/PBLG, and (c) PVPh/PBLG blends.

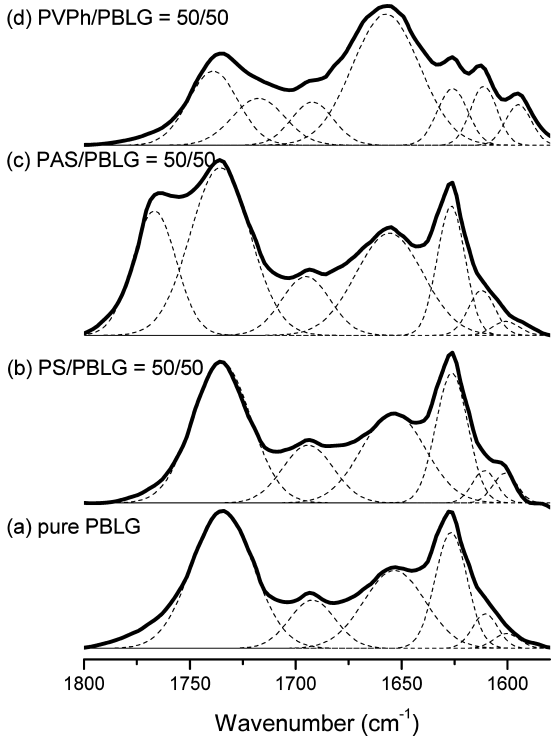

Figure 6. Curve fitting of the signals in the FTIR spectra of the (a) pure PBLG and (b) PS/PBLG = 50/50, (c) PAS/PBLG = 50/50, and (d) PVPh/PBLG = 50/50 blends.

PVPh content at room temperature; it reveals that the fraction of hydrogen-bonded C═O groups on the side chains of PBLG increased upon increasing the PVPh content. Compared with the data for PVPh/PBLG blends reported by Painter et al., the proportion of hydrogen-bonded C═O groups in our PVPh/PBLG blends was negligibly small at most compositions. In our PVPh/PBLG blends, we observed relatively higher fractions of hydrogen-bonded C═O groups of PBLG, presumably because of the molecular weight of our PBLG was much lower than that used by Painter et al. As a result, the more-flexible secondary structures (β-sheet, random coil) were more likely to form intermolecular hydrogen bonds with PVPh than were the rigid α-helical conformations. Therefore, we confirmed that the PVPh/PBLG blend was a miscible system because of the existence of intermolecular hydrogen bonds between the OH groups of PVPh and the C═O groups of PBLG. Next, we determined the corresponding inter- and self-association equilibrium constants for these systems. The self-association constants of PVPh (K_2 = 21.0; K_B = 66.8) had been determined previously.[54] We determined the interassociation constants K_A directly using a least-squares fitting procedure based on the fraction of hydrogen-bonded C═O groups observed experimentally in the PVPh/PBLG blends; using the Painter−Coleman association model, we obtained a value of K_A of 15.[54] This value of K_A for the PVPh/PBLG blends is less than that for the OH···O═C hydrogen-bonding interactions in PVPh/poly(methyl methacrylate) (PMMA) blends (K_A = 37),[54,58] but higher than that in PVPh/poly(L-lactide) blends (K_A = 10),[59] presumably because of the nature of the chemical structure of the group accepting the hydrogen bonds, as has been discussed in detail previously.[60−62]

Figure 8 summarizes the fractions of the secondary structures in the PS/PBLG, PAS/PBLG, and PVPh/PBLG blends at room temperature. It has been reported that at a low DP (<18) both the α-helix and β-sheet secondary structures of PBLG are present, but when the DP increases, the α-helical secondary structure is favored.[1] In this study, we also observed both the α-helix and β-sheet conformations for the PBLG oligomer at a DP of 6. When blended with the PS homopolymer, the fraction of α-helix conformations remained almost unchanged upon increasing the PS content—considerably different from the behavior of PS-*b*-PBLG copolymers. Thus, we observed significant stabilization of the α-helical secondary structure relative to those of the corresponding PBLG oligomers in PS-*b*-PBLG diblock copolymers because of the short-range attraction mediated by covalent bonding between the PS and PBLG segments. When blended with PAS, which can form stronger dipole−dipole interactions, the fraction of the random coil structures of PBLG decreased upon increasing the PAS content, indicating that the presence of PAS stabilized the secondary structures of PBLG. On the other hand, the fraction of α-helical conformations of PBLG increased continuously upon increasing the PAS content. It has been proposed that stacking of the side-chain benzene rings of PBLG plays a role in stabilizing its various structures.[32] Jeon et al. reported that the mobility of the side chain groups of polyglutamates also affects their the α-helical conformations.[63] Their experimental data revealed that longer flexible side chains induced weaker hydrogen bonds between the C═O groups and the amide linkages of the α-helical conformation; a corollary is that rigid benzene rings might enhance hydrogen bonding between the C═O groups and the amide linkages of the α-helical conformation. The dipole−dipole interactions between PBLG and PAS might potentially lead to the PAS coils dissolving in the PBLG domain. Upon increasing the PAS content, the interchain hydrogen bonding of the PBLG segments was initially disrupted, and then intramolecular hydrogen bonding was induced between the PBLG segments; as a result, the content of α-helical conformations increased upon increasing the PAS content. When blended with PVPh, which could form the strongest hydrogen bonds, the fraction of the α-helical conformations of PBLG increased continuously upon increasing the PVPh content—behavior that is similar to that observed

dx.doi.org/10.1021/ma300061w | *Macromolecules* 2012, 45, 2442−2452

Table 2. Curve Fitting of the FTIR Spectroscopic Data for the C═O and Amide Groups in the PS/PBLG, PAS/PBLG, and PVPh/PBLG Blends at 25 °C

	carbonyl group		amide group in PBLG					
	free C═O of PBLG		random coil		α-helix		β-sheet	
PS/PBLG	ν (cm^{-1})	A_f (%)	ν (cm^{-1})	A_f (%)	ν (cm^{-1})	A_f (%)	ν (cm^{-1})	A_f (%)
0/100	1735	100	1692	22.7	1653	45.8	1626	34.5
20/80	1735	100	1692	23.7	1654	42.3	1626	34.0
40/60	1735	100	1694	24.0	1654	40.8	1626	35.2
50/50	1735	100	1694	23.9	1654	41.6	1626	35.5
60/40	1735	100	1693	23.7	1653	41.0	1626	35.3
80/20	1734	100	1690	25.8	1652	38.0	1626	36.2

	carbonyl group				amide group in PBLG					
	PBLG C═O		PAS C═O		random coil		α-helix		β-sheet	
PAS/PBLG	ν (cm^{-1})	A_f (%)	ν (cm^{-1})	A_f (%)	ν (cm^{-1})	A_f (%)	ν (cm^{-1})	A_f (%)	ν (cm^{-1})	A_f (%)
20/80	1735	82.1	1767	17.9	1693	21.2	1654	47.6	1626	31.2
40/60	1735	65.3	1766	34.7	1694	21.1	1655	49.2	1625	29.7
50/50	1735	63.8	1766	26.2	1695	21.2	1655	51.6	1626	27.2
60/40	1735	55.4	1765	44.6	1695	13.6	1660	62.5	1625	23.9
80/20	1731	35.0	1762	65.0			1662	81.9	1625	18.1

	carbonyl group				amide group in PBLG					
	free C═O		HB C═O		random coil		α-helix		β-sheet	
PVPh/PBLG	ν (cm^{-1})	A_f (%)	ν (cm^{-1})	A_f (%)	ν (cm^{-1})	A_f (%)	ν (cm^{-1})	A_f (%)	ν (cm^{-1})	A_f (%)
20/80	1737	76.4	1712	23.6	1692	20.0	1655	55.5	1626	24.5
40/60	1737	65.8	1713	34.2	1691	17.1	1655	63.8	1626	19.1
50/50	1737	60.1	1712	39.9	1692	14.7	1657	71.6	1625	13.7
60/40	1737	49.8	1711	50.2			1658	87.9	1625	12.1
80/20	1737	44.6	1711	55.4			1658	100		

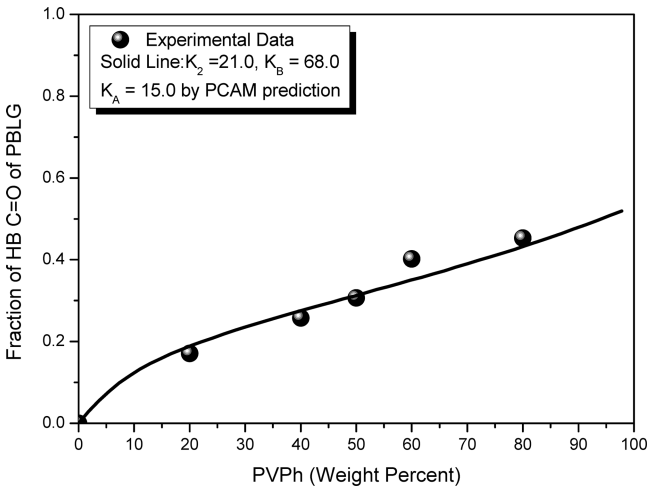

Figure 7. Fractions of hydrogen-bonded C═O groups of PBLG plotted with respect to the PVPh content, with corresponding interassociation equilibrium constants based on the Painter–Coleman association model.

upon adding PAS. Notably, however, the fraction of the α-helical conformations of PBLG in the PVPh/PBLG blend system was higher than that in the PAS/PBLG blends at the same PBLG content. Therefore, the formation of α-helical conformations for PBLG was highly dependent on the strength of the intermolecular interaction. Floudas et al. also noted that suppression of the β-sheet secondary structure of polyalanine (PALa) occurred in PBLG-*b*-PALa copolymers as a result of a thermodynamic field created by the enthalpic interactions of unlike blocks.[64] In our present study, the fraction of α-helical conformations for PBLG was related to the strength of intermolecular interaction, with both following the order PVPh/PBLG (hydrogen bonding) > PAS/PBLG (dipole–dipole) > PS/PBLG (π–π). It is well-established that the α-helical and β-sheet conformations of peptides are stabilized by intra- and intermolecular hydrogen-bonding interactions, respectively. In miscible PVPh/PBLG blends, interchain hydrogen bonding of the PBLG segments initially disrupted and then induced intrachain hydrogen bonding between the PBLG segments upon increasing the PVPh content; as a result, the content of α-helical conformations increased upon increasing the PVPh content.

Solid State NMR Spectroscopic Analyses of Polymer Blends. We also identified the secondary structures of the polypeptides on the basis of their distinctly different resonances in solid state NMR spectra. Figure 9 displays the ^{13}C CP/MAS spectra of the PS/PBLG, PAS/PBLG, and PVPh/PBLG blends at room temperature. The different ^{13}C chemical shifts of the C_α and amide C═O resonances were related to the different local conformations of the individual amino acid residues, characterized by the dihedral angles and their types of intermolecular and intramolecular hydrogen-bonding interactions.[65,66] In the case of pure PBLG, the side chains could stabilize the α-helical secondary structure; the chemical shifts of the corresponding C_α and amide C═O resonances appeared at 57.5 and 176 ppm, respectively. In the β-sheet conformation, these chemical shifts (52.7 and 172 ppm, respectively) were located upfield by approximately 4–5 ppm relative to those for the α-helical conformations.[1,67] Figure 10 provides assignments for the other peaks, as annotated in Scheme 1. From the C═O region of the spectrum of the PS/PBLG blend system, the content of α-helical conformations was almost identical to that

dx.doi.org/10.1021/ma300061w | *Macromolecules* 2012, 45, 2442–2452

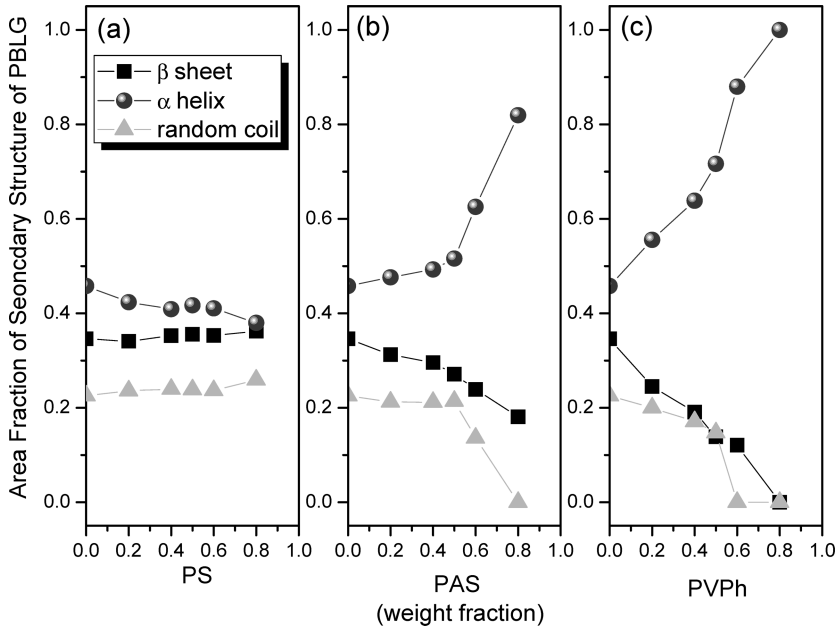

Figure 8. Secondary structures of PBLG in the (a) PS/PBLG, (b) PAS/PBLG, and (c) PVPh/PBLG blends.

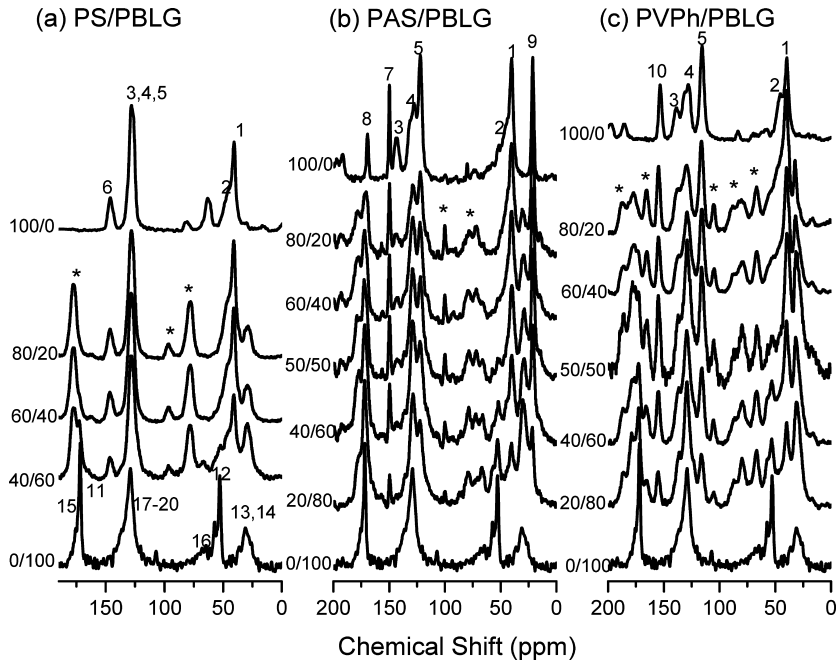

Figure 9. ^{13}C CPMAS spectra (recorded at room temperature) of the (a) PS/PBLG, (b) PAS/PBLG, and (c) PVPh/PBLG blends.

of pure PBLG; in the PAS/PBLG and PVPh/PBLG blend systems, however, the contents of α-helical conformations increased upon increasing the PAS and PVPh contents (Figure 10). In addition, the peak at 153.2 ppm represents the resonance of the phenolic carbon atom of pure PVPh (C-2, Figure 10b);[46−48] we observed a downfield shift of 2.1 ppm for this signal in the PVPh/PBLG = 20/80 blend, relative to that the pure PVPh, implying that intermolecular interassociation occurred between the OH groups of PVPh and the C═O groups of PBLG. We also observed a new peak near 173−174 ppm (downfield to the signals of both the C═O groups and β-sheet of PBLG) in the C═O region, presumably representing the hydrogen-bonded C═O groups. The contribution of a second signal related to the hydrogen-bonded C═O groups is consistent with our observations from the FTIR spectroscopic analyses. Specific interactions in polymer blends can affect the chemical environments of neighboring molecules, resulting in upfield or downfield shifts of the signals representing their resonances.[68,69]

WAXD Analyses of Polymer Blends. We used WAXD at 393 K to identify the secondary structural changes in the PS/PBGL, PAS/PBLG, and PVPh/PBLG blends (Figure 11). Here, we discuss the effects of the strength of the intermolecular interactions between the PS derivatives and PBLG on the type of secondary structure. For pure PBGL at a DP of 6, the diffraction pattern reveals the presence of β-sheet secondary structures. The first peak at a value of q of 0.38 reflects the distance (d = 1.67 nm) between the backbones in

dx.doi.org/10.1021/ma300061w | *Macromolecules* 2012, 45, 2442−2452

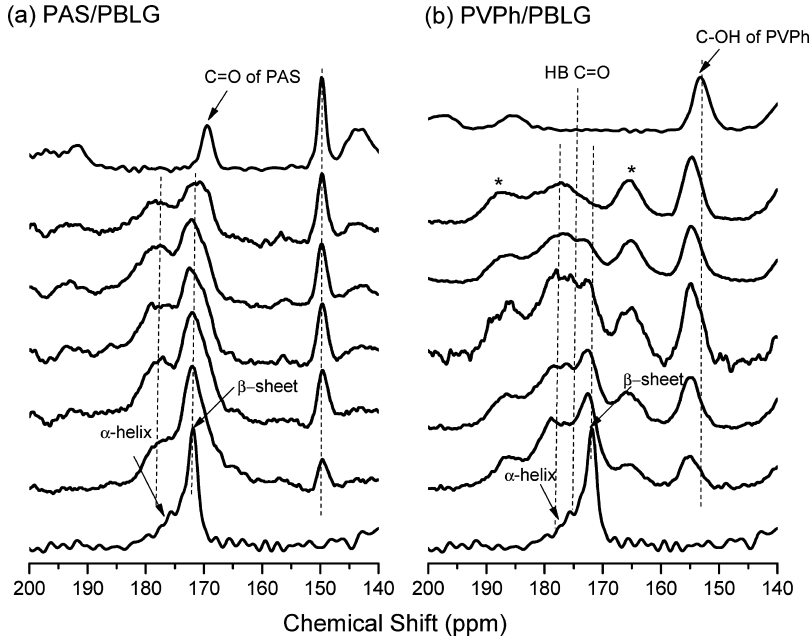

Figure 10. Scale-expanded solid state ^{13}C NMR spectra (displaying signals for the C═O groups) of the (a) PAS/PBLG and (b) PVPh/PBLG blends.

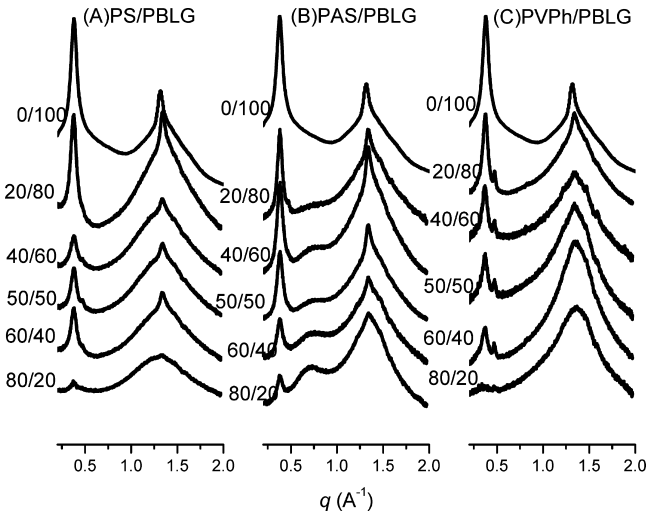

Figure 11. WAXD patterns (recorded at 393 K) of the (a) PS/PBLG, (b) PAS/PBLG, and (c) PVPh/PBLG blends.

the antiparallel β-pleated sheet structure; the reflection at a value of q of 1.34 (d = 0.468 nm) represents the intermolecular distance between adjacent peptide chains within one lamellae, and the broad amorphous region at a value of q of 1.54 originates mainly from the long amorphous side chains.[1] The X-ray patterns at values of q of 0.38 and 1.34 remained almost unchanged upon increasing the PS content, indicating that the secondary structure of PBLG was insensitive to the $\pi-\pi$ interactions occurring with PS, consistent with the conclusions drawn from our analysis of the FTIR spectra. In contrast, the X-ray patterns remained almost unchanged upon increasing the PAS content in the blends; this result differs from that determined from our FTIR spectroscopic analyses, where the α-helical conformation was stabilized, through dipole−dipole interactions, upon increasing the PAS content. We suspect that the conflicting evidence arose because we recorded the WAXD data at a higher temperature (393 K), with the fraction of α-helical conformations decreasing upon increasing the temperature. For the blends with PVPh, which could form the strongest interactions (hydrogen bonds), we observed the appearance of a diffraction peak at a value of q of 0.48, associated with α-helical secondary structures. This feature suggests the presence of that particular conformation in PBLG/PVPh blends, with 2D hexagonal packing of cylinders composed of 18/5 α-helices with a cylinder distance of 1.36 nm.[1] The structure of PBLG has been described as a nematic-like paracrystal with periodic packing of α-helices in the direction lateral to the chain axis. From FTIR spectra, solid state NMR spectra, and WAXD patterns, we obtained the following information regarding the PBLG blends with PS, PAS, and PVPh: (i) for pure PBLG, β-sheet secondary structures are favored; (ii) the α-helical secondary structure is favored for PBLG when dipole−dipole interactions exist with PAS or strong hydrogen bonds occur with PVPh; (iii) weak $\pi-\pi$ interactions with PS do not induce the α-helical secondary structure of PBLG. Thus, the formation of α-helical conformations for PBLG is strongly dependent on the strength of the intermolecular interactions with the functional groups presented on the PS derivatives. Accordingly, even if peptides adopt both α-helical and β-sheet conformations in their pure state, the incorporation of strongly hydrogen-bonding donor polymers (e.g., phenolic resin, PVPh) can induce conformational stabilization, resulting in most of the peptide segments being constrained into the α-helical secondary structures.

Scheme 2 summarizes the possible morphologies, secondary structures, and intermolecular interactions in the blends of PBLG with the PS, PAS, and PVPh homopolymers. The α-helical and β-sheet conformations are stabilized by intra- and intermolecular hydrogen-bonding interactions, respectively. Upon blending with PS, which interacts with PBLG through $\pi-\pi$ stacking, phase separation occurred such that the PS units could not dissolve in the PBLG matrix; because the intra- and intermolecular hydrogen-bonding interactions of PBLG were not disrupted by the PS coils, the secondary structures of PBLG remained almost unchanged upon increasing the PS content.

dx.doi.org/10.1021/ma300061w | Macromolecules 2012, 45, 2442−2452

Because of the stronger dipole−dipole interactions that occurred upon blending with the PAS homopolymer, the PAS coils could dissolve in the PBLG matrix, forming a miscible blend as determined through DSC analysis; thus, the intermolecular hydrogen bonding of PBLG was disrupted in the blends with PAS, favoring greater intramolecular hydrogen bonding of PBLG. That is, the partial fraction of β-sheets transformed into α-helical conformations upon increasing the PAS content. When blending PBLG with PVPh, which could form the strongest noncovalent interactions (hydrogen bonds), we observed phenomena similar to that in the PBLG/PAS system. Notably, however, because the intermolecular interactions with the PVPh coils were stronger than the dipole−dipole interactions with the PAS coils, the fractions of α-helical conformations in the PVPh/PBLG blends were higher than those in the PAS/PBLG blends at the same PBLG content. The fraction of α-helical conformations for PBLG correlated with the strength of the intermolecular interactions, with both increasing in the order PVPh/PBLG (hydrogen bonding) > PAS/PBLG (dipole−dipole) > PS/PBLG ($\pi-\pi$).

CONCLUSIONS

We used ATRP to synthesize homopolymers of three different polystyrene derivatives that we then blended with PBLG to induce changes in its secondary structures. DSC analysis revealed that the PS/PBLG blends were partially miscible, whereas the PAS/PBLG and PVPh/PBLG blends were completely miscible with an amorphous phase over the entire range of compositions. Data obtained from FTIR spectra revealed that the strength of the intermolecular interactions in the blends increased in the order PVPh/PBLG (hydrogen bonding) > PAS/PBLG (dipole−dipole) > PS/PBLG ($\pi-\pi$). FTIR and solid state NMR spectra and WAXD analyses all confirmed that the fraction of α-helical conformations in these three blend systems correlated strongly with the strength of the intermolecular interactions.

AUTHOR INFORMATION

Corresponding Author

*E-mail kuosw@faculty.nsysu.edu.tw; Tel 886-7 5254099.

Notes

The authors declare no competing financial interest.

ACKNOWLEDGMENTS

This study was supported financially by the National Science Council, Taiwan, Republic of China, under Contracts NSC 100-2221-E-110-029-MY3 and NSC100-2628-E-110-003.

REFERENCES

(1) Klok, H. A.; Lecommandoux, S. *Adv. Polym. Sci.* **2006**, *202*, 75.
(2) Yang, J. T.; Doty, P. *J. Am. Chem. Soc.* **1957**, *79*, 761.
(3) Perutz, M. F. *Nature* **1951**, *167*, 1053.
(4) Doty, P.; Bradbury, J. H.; Holtzer, A. M. *J. Am. Chem. Soc.* **1956**, *78*, 947.
(5) Flory, P. J. *Proc. R. Soc. London, Ser. A* **1956**, *234*, 73.
(6) Yang, J. T.; Doty, P. *J. Am. Chem. Soc.* **1957**, *79*, 761.
(7) Perutz, M. F. *Nature* **1951**, *167*, 1053.
(8) Tohyama, K.; Miller, W. G. *Nature* **1981**, *289*, 813.
(9) Prystupa, D. A.; Donald, A. M. *Macromolecules* **1993**, *26*, 1947.
(10) Tohyama, K.; Miller, W. G. *Nature* **1981**, *289*, 813.
(11) Prystupa, D. A.; Donald, A. M. *Macromolecules* **1993**, *26*, 1947.
(12) Kuo, S. W.; Lee, H. F.; Chang, F. C. *J. Polym. Sci., Polym. Chem.* **2008**, *46*, 3108.
(13) Kuo, S. W.; Lee, H. F.; Huang, W. J.; Jeong, K. U.; Chang, F. C. *Macromolecules* **2009**, *42*, 1619.
(14) Papadopoulous, P.; Floudas, G.; Klok, H. A.; Schnell, I.; Pakula, T. *Biomacromolecules* **2004**, *5*, 81.
(15) Klok, H. A.; Lecommandoux, S. *Adv. Mater.* **2001**, *13*, 1217.
(16) Klok, H. A.; Langenwalter, J. F.; Lecommandoux, S. *Macromolecules* **2000**, *33*, 7819.
(17) Sanchez-Ferrer, A.; Mezzenga, R. *Macromolecules* **2010**, *43*, 1093.
(18) Zhou, Q, H.; Zheng, J. K.; Shen, Z. H.; Fan, X, H.; Chen, X. F.; Zhou, Q. F. *Macromolecules* **2010**, *43*, 5367.
(19) Lee, H. F.; Sheu, H. S.; Jeng, U. S.; Huang, C. F.; Chang, F. C. *Macromolecules* **2005**, *38*, 6551.
(20) Papadopoulos, P.; Floudas, G.; Schnell, I.; Aliferis, T.; Iatrou, H.; Hadjichristidis, N. *Biomacromolecules* **2005**, *6*, 2352.
(21) Ibarboure, E.; Rodriguez-Hernandez, J. *J. Polym. Sci., Polym. Chem.* **2006**, *44*, 4668.
(22) Lecommandoux, S.; Achard, M. F.; Langenwalter, J. F.; Klok, H. A. *Macromolecules* **2001**, *34*, 9100.
(23) Crespo, J. S.; Lecommandoux, S.; Borsali, R.; Klok, H. A.; Soldi, V. *Macromolecules* **2003**, *36*, 1253.
(24) Floudas, G.; Papadopoulos, P.; Klok, H. A.; Vandermeulen, G. W. M.; Rodriguez-Hernandez, J. *Macromolecules* **2003**, *36*, 3673.
(25) Hua, C.; Dong, C. M.; Wei, Y. *Biomacromolecules* **2009**, *10*, 1140.
(26) Huang, C. J.; Chang, F. C. *Macromolecules* **2008**, *41*, 7041.
(27) Kong, X.; Jenekhe, S. A. *Macromolecules* **2004**, *37*, 8180.
(28) Kuo, S. W.; Tsai, H. T. *Polymer* **2010**, *51*, 5695.
(29) Lin, Y. C.; Kuo, S. W. *J. Polym. Sci., Part A: Polym. Chem.* **2011**, *49*, 2127.
(30) Hermes, F.; Otte, K.; Brandt, J.; Grawert, M.; Borner, H. G.; Schlaad, H. *Macromolecules* **2011**, *44*, 7489.
(31) Kotharangannagari, V. K.; Sanchez-Ferrer, A.; Ruokolainen, J.; Mezzenga, R. *Macromolecules* **2011**, *44*, 4569.
(32) Painter, P. C.; Tang, W. L.; Graf, J. F.; Thomson, B.; Colema, M. M. *Macromolecules* **1991**, *24*, 3929.
(33) Asano, A.; Kurotu, T. *J. Mol. Struct.* **1998**, *441*, 129.
(34) Murata, K.; Katoh, E.; Kuroki, S.; Ando, I. *J. Mol. Struct.* **2004**, *689*, 223.
(35) Deng, X.; Hao, J.; Yuan, M.; Xiong, C.; Zhao, S. *Polym. Int.* **2001**, *50*, 37.
(36) Aoi, K.; Nakamura, R.; Okada, M. *Macromol. Chem. Phys.* **2000**, *201*, 1059.
(37) Kuo, S. W.; Chen, C. J. *Macromolecules* **2011**, *44*, 7315.
(38) Kuo, S. W.; Huang, W. J.; Huang, C. F.; Chan, S. C.; Chang, F. C. *Macromolecules* **2004**, *37*, 4164.
(39) Sheen, Y. C.; Lu, C. H.; Huang, C. F.; Kuo, S. W.; Chang, F. C. *Polymer* **2008**, *49*, 4017.
(40) Huang, K. W.; Tsai, L. W.; Kuo, S. W. *Polymer* **2009**, *50*, 4876.
(41) Daly, W. H.; Poche, D. *Tetrahedron Lett.* **1988**, *29*, 5859.
(42) Kuo, S. W.; Huang, C. F.; Lu, C. H.; Lin, H. M.; Jeong, K. U.; Chang, F. C. *Macromol. Chem. Phys.* **2006**, *207*, 2006.
(43) Kuo, S. W.; Huang, C. F.; Tung, P. H.; Huang, W. J.; Huang, J. M.; Chang, F. C. *Polymer* **2005**, *46*, 9348.
(44) Kuo, S. W.; Chang, F. C. *Polymer* **2001**, *42*, 9843.
(45) Kuo, S. W.; Chang, F. C. *Macromol. Chem. Phys.* **2002**, *203*, 868.
(46) Kuo, S. W.; Chang, F. C. *Macromolecules* **2001**, *34*, 4089.
(47) Kuo, S. W.; Chang, F. C. *Macromolecules* **2001**, *34*, 5224.
(48) Kuo, S. W.; Tung, P. H.; Chang, F. C. *Macromolecules* **2006**, *39*, 9388.
(49) Lodge, T. P.; Wood, E. R.; Haley, J. C. *J. Polym. Sci., Part B: Polym. Phys.* **2006**, *44*, 756.
(50) Lodge, T. P.; Mcleish, T. C. B. *Macromolecules* **2000**, *33*, 5278.
(51) Papadopoulos, P.; Floudas; Schnell, I.; Klok, H. A.; Aliferis, T.; Iatrou, H.; Hadjichristidis, N. *J. Chem. Phys.* **2005**, *122*, 224906.
(52) Fox, A.; Loshaek, S. *J. Polym. Sci.* **1955**, *15*, 371.
(53) Barclay, G. G.; Hawker, C. J.; Ito, H.; Orellana, A.; Malenfant, P. R. L.; Sinta, R. F. *Macromolecules* **1998**, *31*, 1024.

(54) Coleman, M. M.; Graf, J. F.; Painter, P. C. *Specific Interactions and the Miscibility of Polymer Blends*; Technomic Publishing: Lancaster, PA, 1991.
(55) Coleman, M. M.; Painter, P. C. *Prog. Polym. Sci.* **1995**, *20*, 1.
(56) Coleman, M. M.; Painter, P. C. *Polymer Blend*; Paul, D. R., Bucknall, C. B., Eds.; Wiley: New York, 2000.
(57) Surewicz, W. K.; Mantsch, H. H. *Biochim. Biophys. Acta* **1988**, *952*, 115.
(58) Lin, C. L.; Chen, W. C.; Liao, C. S.; Su, Y. C.; Huang, C. F.; Kuo, S. W.; Chang, F. C. *Macromolecules* **2005**, *38*, 6435.
(59) Kuo, S. W. *J. Polym. Res.* **2008**, *15*, 459.
(60) He, Y.; Zhu, B.; Inoue, Y. *Prog. Polym. Sci.* **2004**, *29*, 1021.
(61) Lin, C. T.; Kuo, S. W.; Chang, F. C. *J. Phys. Chem. B* **2010**, *114*, 1603.
(62) Kuo, S. W.; Lin, C. T.; Chen, J. K.; Ko, F. H.; Chang, F. C.; Jeong, K. U. *Polymer* **2011**, *52*, 2600.
(63) Jeon, S.; Choo, J.; Sohn, D.; Lee, S. N. *Polymer* **2001**, *42*, 9915.
(64) Gitsas, A.; Floudas, G.; Mondeshki, M.; Spiess, H. W.; Aliferis, T.; Iatrou, H.; Hadjichristidis, N. *Macromolecules* **2008**, *41*, 8072.
(65) Murata, K.; Katoh, E.; Kuroki, S.; Ando, I. *J. Mol. Struct.* **2004**, *689*, 223.
(66) Kricheldorf, H. R.; Muller, D. *Macromolecules* **1983**, *16*, 615.
(67) Floudas, G.; Spiess, H. W. *Macromol. Rapid Commun.* **2009**, *30*, 278.
(68) Huang, M. W.; Kuo, S. W.; Wu, H. D.; Chang, F. C.; Fang, S. Y. *Polymer* **2002**, *43*, 2479.
(69) Hill, D. J. T.; Whittaker, A. K.; Wong, K. W. *Macromolecules* **1999**, *32*, 5285.